Available online at www.CivileJournal.org

Civil Engineering Journal

(E-ISSN: 2476-3055; ISSN: 2676-6957)

Vol. 7, Special Issue, 2021

"Innovative Strategies in Civil Engineering Grand Challenges"

Behavior of Reinforced Concrete Deep Beams with Openings under Vertical Loads Using Strut and Tie Model

Rasha T. S. Mabrouk [1*], Mahmoud A. S. Mahmoud [2], Magdy E. Kassem [1]

[1] *Structural Engineering Department, Faculty of Engineering, Cairo University, Cairo, Egypt.*

[2] *Faculty of Engineering, Cairo University, Cairo, Egypt.*

Received 09 February 2022; Revised 14 April 2022; Accepted 26 April 2022; Published 11 May 2022

Abstract

This research aims to study the effects of the size and location of openings on deep beams. The analysis of deep beams with openings presents a rather complex problem for engineers, as there are currently no guidelines within the design codes for this problem. Using the strut and tie model is a feasible solution, but also gives some uncertainties due to the various models that can be used. This paper proposes using a strut and tie model for the deep beams with openings where reinforcement is laid out in the form of embedded struts and ties. The study is divided into an experimental and a numerical part. The experimental study was conducted on eight reinforced concrete deep beams under vertical loads. Seven of the beams had web openings of different sizes and locations, while the eighth specimen was a reference beam without any openings. The beams had the same concrete dimensions with the size of the openings in the web taken as 150×150 mm and 300×300 mm, and the location of the opening in the horizontal direction was varied between 0.11 to 0.4 the span. The experimental results were analyzed in terms of cracking pattern, mode of failure, and load-deflection behavior and then compared to numerical analysis conducted using a finite element program. A parametric study followed to investigate the influence of reinforcement arrangement and reinforcement around the openings on the behavior of deep beams. The results showed that large web openings that directly interrupted the compression strut had the most reduction in beam capacity and that the location of the opening did not significantly affect the strength of the beam in the case of small openings.

Keywords: Deep Beam; Strut and Tie Model; Finite Element Analysis; Web Opening; Strut Reinforcement.

1. Introduction

Reinforced concrete deep beams are typically used in high rise buildings and bridges as transfer girders as well as in offshore structures. Deep beams are generally defined by the design codes according to the ratio of the span to the height of the beam or the shear span to depth ratio. ACI 318-19 [1] defines deep beams as having a clear span that does not exceed 4 times the overall member depth (h) or that the concentrated loads exist within a distance of 2h from the face of the support. The Egyptian code of practice ECP 203-18 [2] defines deep beams as having an effective span to effective depth ratio of less than or equal to 4. Shear behavior is usually the governing factor controlling the strength of the deep beams. However, Bernoulli's hypothesis for the standard design of structural elements cannot be applied in this case as the entire deep beam acts as discontinuity regions (D regions) [3]. Therefore, design using nonlinear strain distribution, or the strut and tie model (STM), which follows the lower bound theorem of plasticity, is recommended to be used. However, the design using the nonlinear strain distribution is rather complicated and thus the use of STM is more

* Corresponding author: yrasha@yahoo.com

http://dx.doi.org/10.28991/CEJ-SP2021-07-011

commonly used. The cracked D-regions are analyzed where the continuous principal compressive and tensile stress fields are represented using discrete struts and ties. The struts and ties are interconnected at nodes. Most design codes, such as ACI 318-19 [1], Eurocode 2 [4], CEB-FIP [5], CSA A23.3-19 [6], and the Egyptian Code of Practice ECP 203-18 [2], permit the use of STM.

With such large elements like deep beams, the need for openings usually arises to allow for the passage of ducts, pipes, or other utility elements. The presence of openings in the web area of deep beams affects their overall behavior where the shear strength is considerably reduced due to the stress concentration at the corners of the openings. In this case, the STM becomes more complicated than in the case of the simple solid deep beam due to the discontinuity caused by the opening, which affects the path of the compression struts. The compression strut from the area of loading going towards the supports usually separates around the openings before coming together again beyond the openings. In this case, the ultimate capacity of the beam is largely affected by the size and location of the opening [3].

Lots of research and international design codes have dealt with the design and detailing of reinforced concrete deep beams without openings, whether for the prediction of their shear capacity [7-10] or the evaluation of the limitations of applying the different design code specifications [11, 12]. In addition, alternative modeling techniques were proposed where Elzoughiby [13] used a simple method to define the load distribution in deep beams under different types of loads, while Hwang et al. [14] proposed a softened STM which can be used to compute the shear capacity of deep beams with a shear span to depth ratio of less than 2. Lee et al. [15] proposed a model that can solve the deep beams with openings by simplifying that given by the ACI 318-19 [1] where it can reduce the complex calculations needed.

Parallel research has been conducted for deep beams with openings since the early 70^{th} where Kong and Sharp [16] introduced a structural idealization for the problem of deep beams with openings. In their formulation the load is assumed to take two paths; a lower and an upper one and formulae were given for the computation of the shear capacity. Their work was later asserted by Kong et al. [17] where more evidence was presented to support their idea. Although design codes support the use of strut and tie model for the design of deep beams, no provisions or guidelines were given for deep beams with openings. However, research articles widely studied the STM in case of openings in deep beams. Almeida and Oliveira Pinto [18] experimentally studied three high strength concrete deep beams with openings where they compared the results obtained using the strut and tie model and various equations available for the design of deep beams with openings. They concluded that the available equations as well as the STM did not give good results compared to the experiment and the STM was complicated to use. On the other hand, Maxwell and Breen [19] studied four variations of the STM using four deep beams with large openings. They showed that the specimens performed very similarly to the assumed STM and that the strut and tie model can be a useful tool in dealing with deep beams with openings. Eun et al. [20] tested eighteen beams with variable parameters namely the steel ratio, strength of longitudinal bars, concrete strength, and shear span-to-depth ratio. They proposed a modified model based on the softened truss model of Mau and Hsu [21]. Ley et al. [22] examined different proposed strut and tie models using simple supported dapped beams. The beams were tested under three-point loading and the results showed that despite using different strut and tie models, all beams yielded safe conservative results which assert the flexibility and usefulness of the STM. Garber et al. [23] extended the use of strut and tie model to statically indeterminate deep beam. Four test specimens each having three openings and designed according to four different strut and tie models were tested. They concluded that STM can be effectively used with indeterminate structures giving a conservative solution. They also observed that the load path depends on the used detailing of reinforcement.

Although using the STM presents a flexible and vital tool in the design of deep beams with opening, it also presents a challenge where there is no one solution available. Brena and Morrison [24] presented the results of four deep beams with openings designed using different strut and tie models. They aimed at evaluating the amount of conservativeness of the strut and tie model and the source and amount of over strength obtained experimentally compared to the STM. The concluded that the failure load obtained from experiments occurred at much higher values than the calculated capacities with ratios varying between 1.7 and 3.2. Zhou et al. [25] aimed to evaluate the different available models for the same discontinuity region to decide upon which can be a more appropriate model to be used. They concluded that their evaluation system can successfully rate the performance of different strut and tie models developed from the same member. In addition, different authors tried to provide tools for the automatic generation of the strut and tie model where Vaquero and Bertero [26] tried to propose an automatic tool for the generation of strut and tie model that can be easy to be used and requires low input from the designer which can help in the design process. El-Zoudhiby [27] proposed an approach to generate the strut and tie model for deep beams with openings based on the load path criteria where he verified his method by the generation of the strut and tie models for well-known problems. Tan et al. [28] also proposed an approach to study deep beams with openings having different opening size and locations and different web reinforcement arrangements.

The location and size of the openings largely affect the behavior of the deep beams. Ashour and Rishi [29] studied sixteen two span deep beams having openings with variable location and size. The web reinforcement arrangement was also a parameter under study where the beams were divided into four groups: one with only vertical bars, one with only horizontal bars and two groups with meshes of horizontal and vertical bars. They concluded that the mode of failure depended on the location of the opening and that the vertical web reinforcement affected the strength of the beams more than the horizontal ones. Campione et al. [30] studied the effect of circular openings on deep beams. They studied the position of the opening and different arrangement of web reinforcement in the vertical and horizontal directions and concluded that the effect of the opening on the behavior of the beam depends on the opening location. Frappier et al. [31] studied the behavior of seven deep beams with openings. The beams were reinforced either with glass fiber-reinforced polymer (GFRP) bars or ordinary steel bars as web reinforcement around the opening using different arrangements.

Yang et al. [32] also studied the location of openings in deep beams and different arrangements of inclined web reinforcement. They proposed an effective factor considering the size of the opening and the web reinforcement ratio. Yang et al. [33] extended the study to twenty-two reinforced concrete continuous deep beams with openings. The parameters under study were the configuration of web reinforcement around openings, location of openings, and shear span-to-overall depth ratio.

Some research articles discussed the feasibility of using finite element analysis to deal with the complexity of deep beams with opening. Jasim et al. [34] conducted an experimental and analytical study on five deep beams having openings with different arrangements and sizes. According to their study the finite element program gave un-conservative results. Starčev-Ćurčin et al. [35] used the software "ST method" to obtain the strut and tie models for three deep beams with openings with the aim of finding the optimum model. Ibrahim et al. [36] presented an analytical model for deep beams with openings and verified it through previous experimental data. A finite element analysis was conducted where they studied opening size and location as well as different reinforcement arrangement around the web including the use of embedded struts. The finite element analysis gave good correlation with the experimental data, and they also concluded that using embedded strut was more beneficial in case of an inclination angle more than 30º.

Based on the above, research was conducted on deep beams with opening with much focus on the different strut and tie models where reinforcement arrangement around the opening followed some assumed strut and tie model. However, not much research studied the effect of the size and location of openings on the behavior of deep beams. And for most of this research the reinforcement arrangement used around the opening was variation of the regular orthogonal web mesh. This research focuses on the effect of the size and location of the opening and at the same time uses a simple reinforcement layout based on the strut at tie model where the force is diverted using reinforcing bars placed around the opening. Using horizontal and vertical bars as web reinforcement is easier to construct but it does not represent the actual force flow along the height of the beam. Tan et al. [38] and Tseng et al. [37] proposed that the force flow follows an upper and a lower path around the opening. This research builds on this idea for the reinforcement details and aims to study the effect of the size and location of openings.

An experimental program is conducted where a simple reinforcement configuration using embedded struts connecting the loading point to the supports is investigated. Struts are reinforced using inclined reinforcement and stirrups are added to the struts to supply proper confinement to the concrete and thus help to resist strut crushing. In addition, longitudinal reinforcement is placed in the direction of the lower horizontal tie. The arrangement is used for all specimens with additional reinforcement placed around the openings. Following that an analytical study is performed. Few research was conducted based on the use of finite element analysis for deep beams with openings. So in addition, this research aims to further investigate the finite element simulation as a tool that can be used to analyze deep beam with openings.

2. Research Significance

The size and location of an opening as well as the reinforcement arrangement significantly affects the behavior of deep beams. This paper presents an experimental and analytical study to study the behavior of deep beams with opening. Eight deep beams were tested with varying opening sizes, locations, and using two embedded strut reinforcement layouts. The beams were chosen to have one opening on one side and loaded under one point load which is different from the previous conventional test setups. The behavior of the tested beams was assessed and compared with the results of the finite element model used. A parametric study was also conducted to compare the conventional mesh reinforcement layout with the proposed strut arrangement used in the tested beams as well as the effect of the additional reinforcement used around the openings. Figure 1 gives a flowchart showing a summary of this research program.

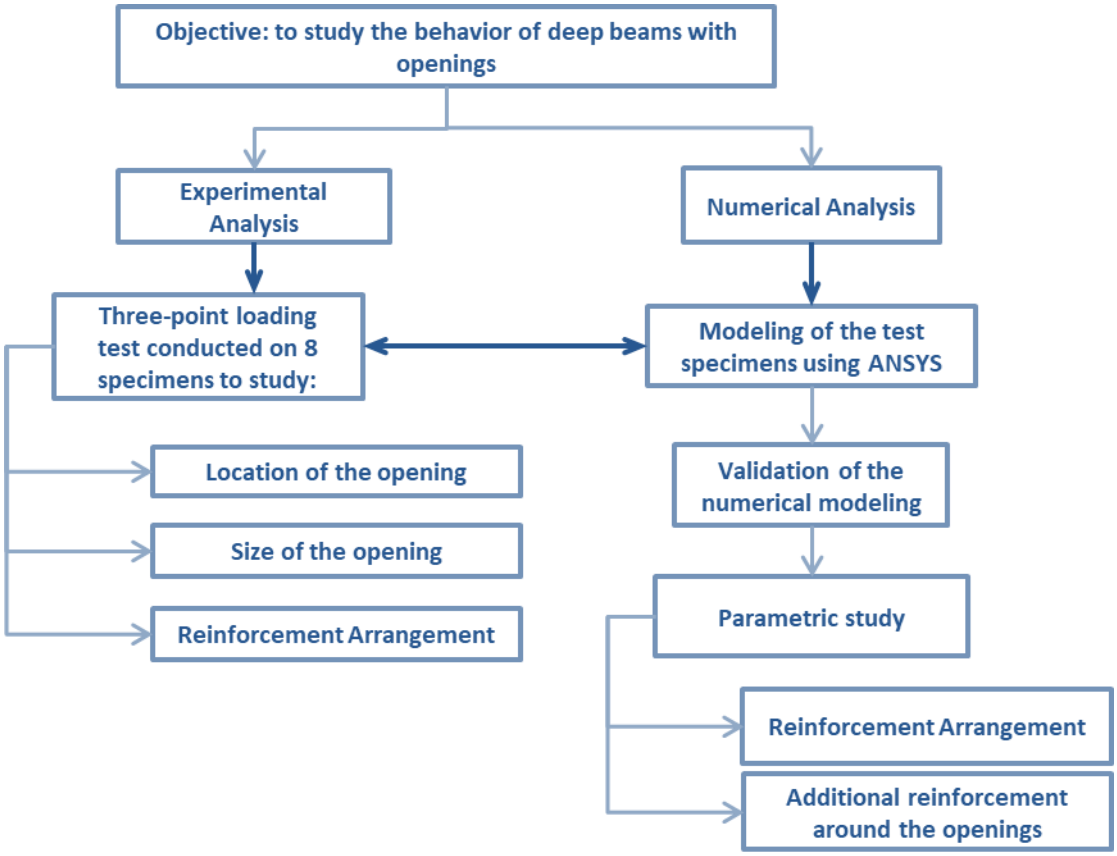

Figure 1. Layout of the research program

3. Experimental Program

3.1. Beam details

The experimental program consisted of testing eight deep beams under one point loading system at the Concrete Research Laboratory, Faculty of Engineering, Cairo University. The details of the eight deep beams are shown in Table 1.

Table 1. Details of the specimens used in experimental program

Group	Beam	Dimensions (mm)	Opening size (mm)	m_1*	m_2*	m_1m_2**	Opening center line location		Reinforcement arrangement
							Horizontal	Vertical	
A	A	2000*1000*150	-	-	-	-	-	-	Type I
B	B1		150*150	0.167	0.15	0.025	0.11 L	0.5h	Type I
	B2		300*300	0.333	0.30	0.100	0.11 L		Type I
C	C1		150*150	0.167	0.15	0.025	0.22 L		Type I
	C2		300*300	0.333	0.30	0.100	0.22 L		Type I
	C3		150*150	0.167	0.15	0.025	0.22 L		Type II
D	D1		150*150	0.167	0.15	0.025	0.40 L		Type I
	D2		300*300	0.333	0.30	0.100	0.40 L		Type I

m_1* = Opening width/shear span, m_2* = Opening height/ beam height, m_1m_2** = Opening area/shear span area

All beams had the same dimensions of 1000 × 150 mm cross section and a length of 2000 mm giving a clear span of 1800 mm. The first beam, denoted beam A, was a reference specimen without any openings. A truss model that satisfies equilibrium with the applied load was chosen where two inclined struts are assumed from the loading point to the two supports with a horizontal tie connecting the two struts at the lower fiber of the beam. The reinforcement arrangement in this research is taken following the truss model assumed instead of the conventional simplified orthogonal pattern as shown in Figure 2 where reinforcement in the direction of the two compression struts and the tie is used. The strut and tie model was used to determine the amount and distribution of reinforcement in the concrete members. The main longitudinal bottom reinforcement was two steel bars of 25 mm diameter. The bottom reinforcement

representing the horizontal tie extended the full length and then into the depth of the beams to provide sufficient anchorage. The longitudinal top reinforcement was two steel bars of 12 mm diameter. The reinforcement of the two embedded struts was four bars with diameter 12 mm as a compression reinforcement and 5 Ø 6 /m as stirrups to carry the transverse tensile strain developed within the struts. A mesh reinforcement of 5 Ø 6 /m for each side of the beam was also used. As the aim of the research is to investigate the reinforcement in the direction of the struts and tie, the orthogonal mesh reinforcement was added just for practical consideration during casting of the specimens and the value of mesh reinforcement ratio was chosen lower than the recommended minimum value to assure it did not influence the overall behavior of the beams. The details of beam A are given in Figure 3.

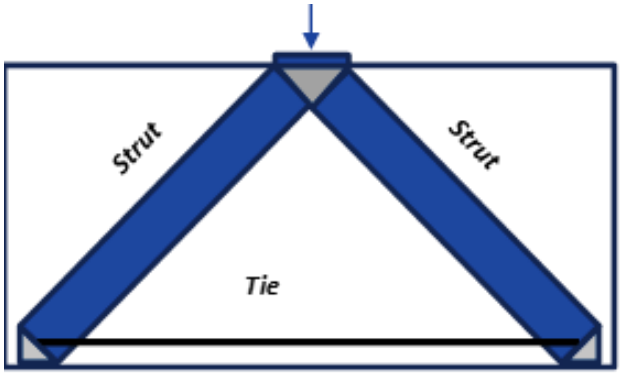

Figure 2. Strut and tie model used

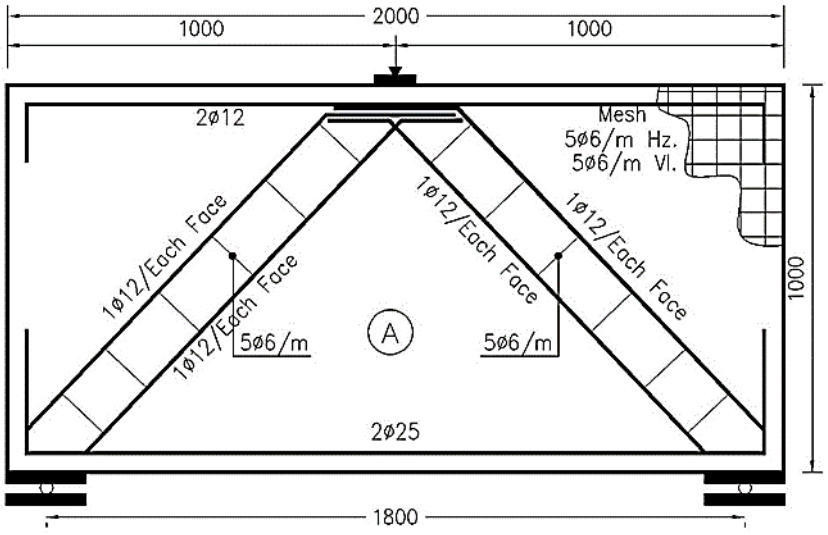

Figure 3. Details of control specimen Beam A. (Dimensions are in mm)

The other seven beams were cast with one web opening on one side where the location of opening was selected to interrupt the load flow from the load to the end support at different locations. It has been reported previously that the decrease in the beam strength depends largely on the location of the opening and the degree it interrupts the load path through the compression struts [20, 30]. Following that this research aims to investigate different locations of the web openings as well as the effect of the opening size for the different locations. The vertical location was kept constant where the center line of the opening was at mid height of the beams. Three values were chosen for the horizontal location of the opening where it interrupts the compression strut with varying extents. The beams with openings were divided into three groups B, C, and D according to the horizontal location of the center line of openings. Group B had the center line of the opening at 300 mm from the edge of the beam representing a ratio of 0.11 L where L is the clear span of the beam. In Group C, the opening was located at 500 mm from the edge, or 0.22 L and group D was at 800 mm from the edge giving a ratio of 0.4 L as shown in Figure 4. Group C represents web opening directly interrupting the path of the compression strut while Group B has openings just to the outer side of the beam towards the supports and group D towards the middle of the beam. For each group two beams with two opening sizes were studied. Small openings of size 150×150 mm giving an opening width/shear span of 0.167 and opening height/beam height of 0.15 and larger openings of size 300×300 mm giving an opening width/shear span of 0.333 and opening height/beam height of 0.3. These two sizes were chosen to represent ratios of opening area to shear span area of 0.025 and 0.1. For ease of reference, the four corners of the openings are referred to as a, b, c, and d while the loading point is labeled point p and the two supports S1 and S2.

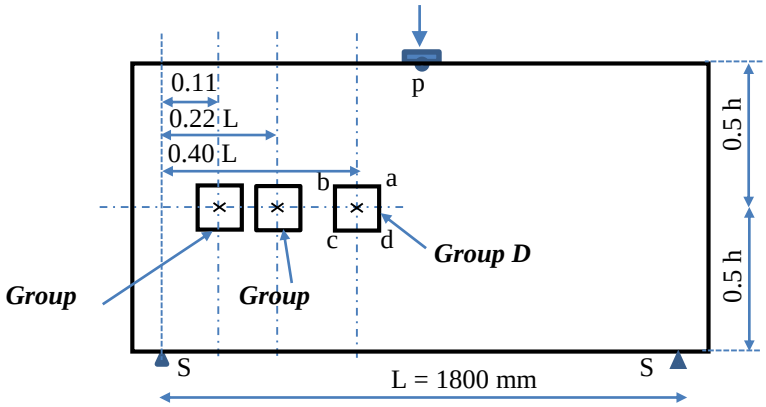

Figure 4. Different locations of the web opening

The same amount of the main longitudinal bottom and top reinforcement as well as the meshes on both sides used for beam A was also used for the beams with openings. The amount of reinforcement of the two struts was also same for the beams, however, two types of reinforcement layouts were used. The first one will be named here in as Type I where the detailing of the strut around the openings was kept following the path of the compression strut and just adjusted to give enough development lengths as needed around the openings where they interrupted the strut as shown in Figure 5. This pattern was used for beams B1, B2, C1, C2, D1 and D2 and these beams details are shown in Figure 6. For beam C3 the second type was used herein named as Type II. In this case instead of the strut reinforcement directly interrupted by the opening the reinforcement was diverted around the opening on the lower side as shown in Figure 7. The lower path was chosen as Tseng et al. [37] reported that the upper path is not effective if there is no web reinforcement above the opening and that the lower path is always available. In addition, two steel bars of diameter 12 mm were used around each of the four sides of the opening in all the beams with openings.

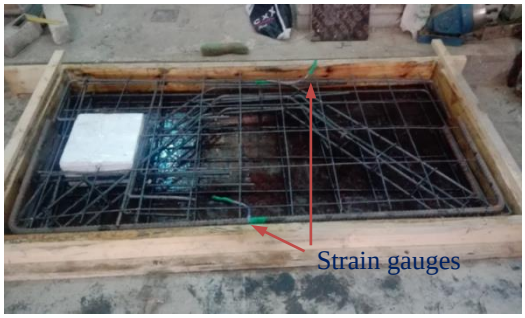

Figure 5. Reinforcement layout of one beam with opening (Type I)

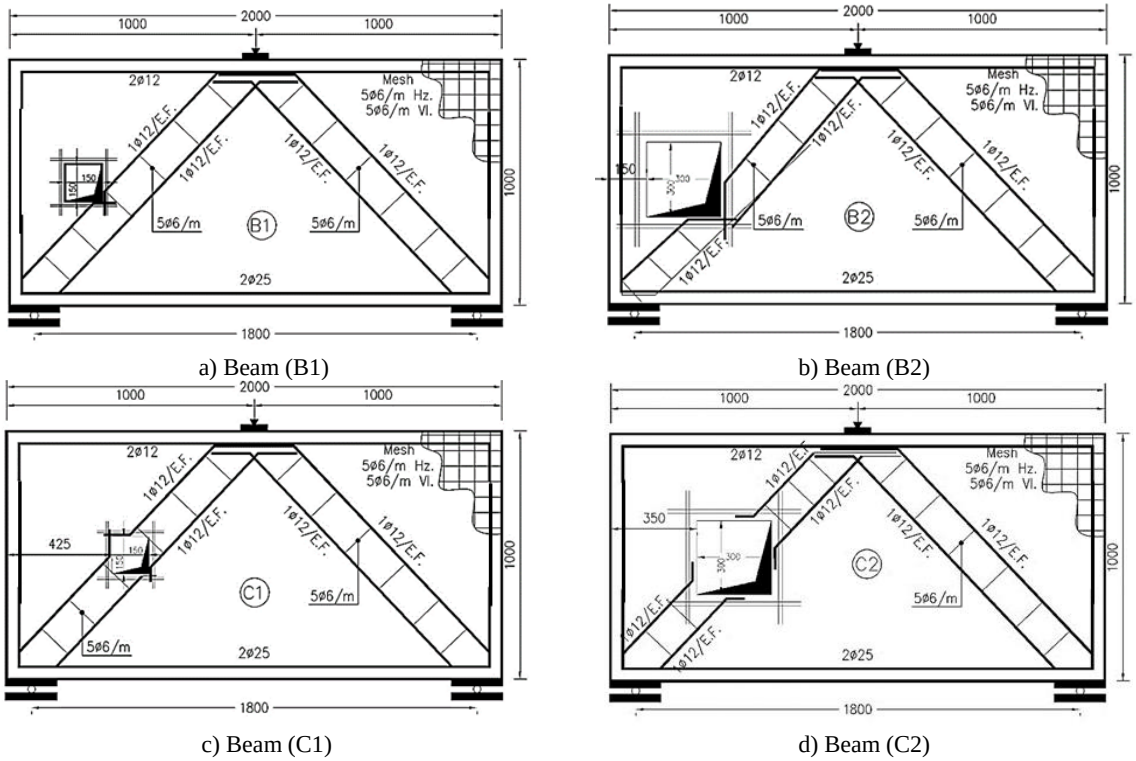

a) Beam (B1)

b) Beam (B2)

c) Beam (C1)

d) Beam (C2)

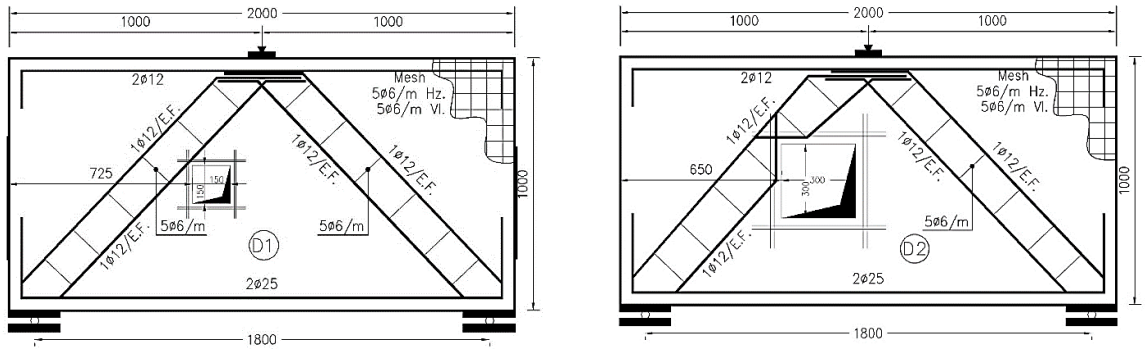

e) Beam (D1) f) Beam (D2)

Figure 6. Details of beam specimens with openings (Type I). (Dimensions are in mm)

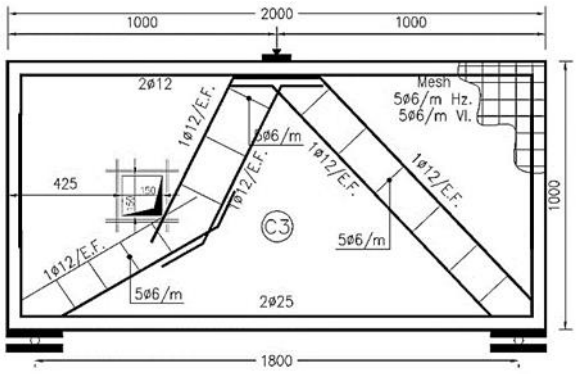

Figure 7. Reinforcement details of beam C3 (Type II). (Dimensions are in mm)

3.2. Materials and Test Setup

The concrete mix used for the beams was designed to give characteristic compressive strength of 30 MPa after 28 days. The absolute volume method was used to determine the concrete mix proportions. For every beam, 3 cubes with dimensions 150×150×150 mm were prepared during casting. The compression test for concrete cubes was done to ensure the required concrete compressive strength where the results gave an actual average compressive strength of 35 MPa after 28 days. High-grade steel (360/520) was used for the main strut as well as longitudinal top and bottom reinforcement while mild steel (240/360) was used for the additional reinforcement around openings. Two electrical resistance strain gauges were used in each beam to measure the strain in the top and bottom main reinforcement as shown in Figure 5. The specimens were cured for 28 days and after that they were tested using a one-point load system. The specimens were mounted on the testing machine, where the clear span between the two supports was kept at 1800 mm. A 5000 kN capacity hydraulic loading jack was used for loading the deep beam specimens and the deflection at mid span was recorded using linear variable displacement transducers (LVDTs) up to the failure load.

4. Experimental Results and Discussion

4.1. Cracking Patterns and modes of Failure

The cracking pattern for the control beam A is shown in Figure 8. The first crack observed was an almost vertical flexural crack near midspan at 550 kN which represents around 50 % of the ultimate load capacity. As the loading increased flexural shear cracks formed on both sides of the beam together with some flexural cracks at the bottom soffit of the beam. Following that, another pair of distinct diagonal cracks extended from the supporting plates to the loading plate until failure finally occurred across the strut going towards the right support. Just before failure, the beam had almost symmetric crack pattern along the two sides of the beam. However, failure occurred along one side as pure symmetry is quite difficult to maintain during the experimental testing of the beam.

Figures 9 and10 show the cracking pattern for groups B, C, and D where the beams had web openings with two different sizes and different locations. The seven beams had a different cracking pattern from the control beam A. The change in the horizontal location of the web opening did not significantly affect the first crack or the failure mode of the beams but the size of the opening did. For beams B1, C1, C3, and D1 having the smaller opening size with m_1m_2= 0.025, the first crack was observed along the diagonal strut extending from the support towards the loading plate. For beam B1, it occurred on the same side as the opening from S2 towards P and occurred on the opposite side to the opening from S1 to P for beams C1, C3, and D1 at different loading levels. For beams B2, C2, and D2 with the larger opening size of m_1m_2= 0.1, the first crack was generally observed starting from the corners of the opening a and c. For beam B1 it extended from corner a towards the loading point P and from corner c to the supporting plate S2. For C2 and D2 cracks were also observed along the sides of the opening as shown in Figure 9.

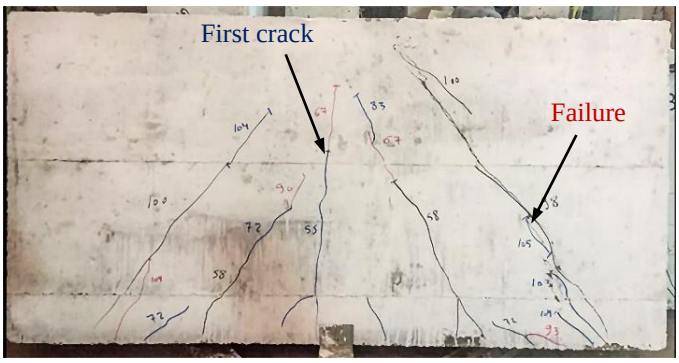

Figure 8. Cracking pattern for Beam A at failure

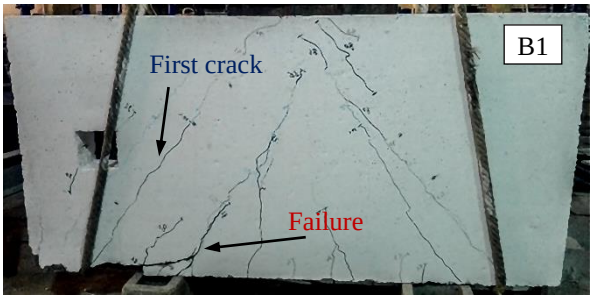

a) Beam (B1)

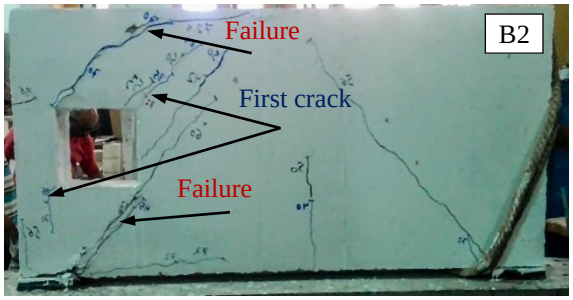

b) Beam (B2)

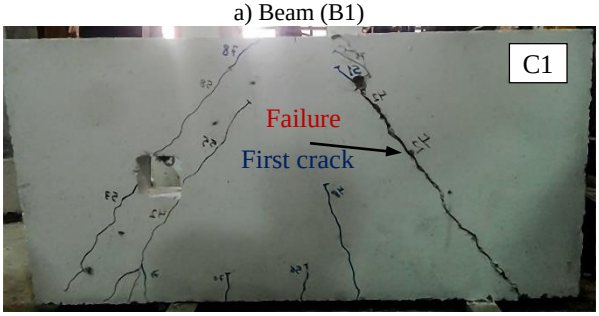

c) Beam (C1)

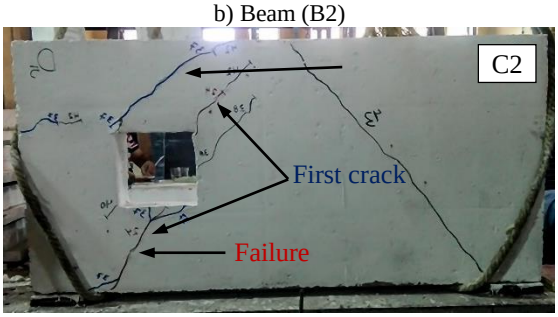

d) Beam (C2)

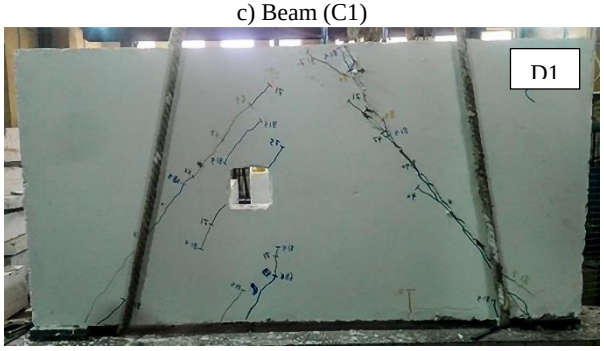

e) Beam (D1)

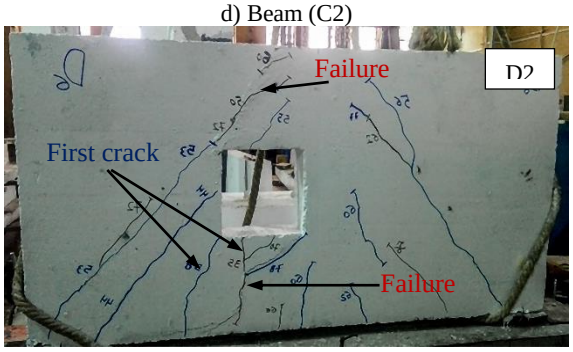

f) Beam (D2)

Figure 9. Cracking patterns of specimens with opening at failure

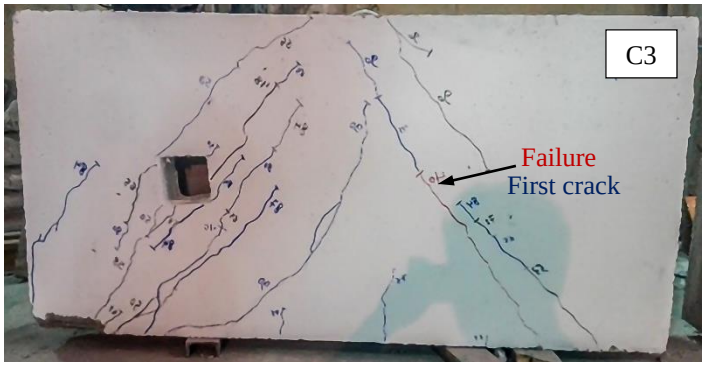

Figure 10. Cracking patterns of specimen C3 at failure

Flexural cracks occurred in all beams except for beam C2. The flexural cracks were seen at about 65% of the ultimate load for beams B1 and C1 and at 84% for beam D1. While it was recorded at 55% for beam B2 and at 75% for beam D2. For Beam C3, where an alternate strut reinforcement layout was used compared to beam C1, more flexural shear cracks were seen around the middle part of the beam as well as more dispersed crack patterns were observed around the web opening.

Various modes of failure of RC deep beams are reported in the literature such as shear compression, shear tension, local crushing near the support and loading points, compression strut failure, flexural failure, or diagonal tension failure [38]. Two modes of failure were observed for the beams with small openings. For beam B1, shear tension failure occurred where a tensile crack in the region of combined flexure and shear propagated into diagonal shear crack extending almost to half the beam depth towards the loading point P. This crack also propagated backward along the longitudinal reinforcement causing loss of bond and splitting of the concrete at the support. The splitting of concrete could be due to concrete crushing occurring over the support. In some situations, some unpredicted horizontal confinement can occur at the support leading to very high stresses. Careful attention needs to be given to the detailing of these areas in future research. For beams C1, D1, and C3, compression failure along the strut connecting the loading and supporting points was observed. For beams with large openings, one distinct mode of failure was observed where shear compression failure occurred along diagonal cracks that propagated from the corners of the opening b and d and extended till reaching the loading plate P and the end support S2.

4.2. Load and Deflection

Table 2 shows the experimental data recorded, namely first cracking loads, ultimate loads, and deflection of the tested beams. Figures 11 to 14 show the load deflection curves for the different beam groups. The load deflection curves followed similar patterns and can be generally divided into three parts. The first part can be observed at the lower levels of loading where the load deflection curves were linear. As the load increased, cracking started to propagate causing a reduction in the stiffness of the beams and thus the slope of the load deflection curve started to decrease until the ultimate load occurred. Following that the third part of the curve was observed in all the beams except for group C. In this part excessive cracks are present and tension softening can be clearly seen. Figures 12 and 14 show that Group C had the most brittle behavior with the lowest deflection measured at mid span among the three groups and a rather sudden failure was observed.

Table 2. Experimental results of tested specimens

Group	Beam	Opening area ratio	Opening location	First flexural cracking load (kN)	First diagonal cracking load at corners of opening (kN)	First diagonal cracking load along compression strut (kN)	Ultimate Load (KN)	Deflection at Ultimate Load (mm)
A	A	-	-	550	-	580	1043	3.64
B	B1	0.025	0.11 L	560	500	385	866	4.73
	B2	0.100	0.11 L	400	310	320	724	2.84
C	C1	0.025	0.22 L	480	420	420	789	2.89
	C2	0.100	0.22 L	-	240	240	468	2.59
	C3	0.025	0.22 L	680	500	400	891	1.86
D	D1	0.025	0.40 L	686	710	385	817	3.72
	D2	0.100	0.40 L	600	380	440	792	3.76

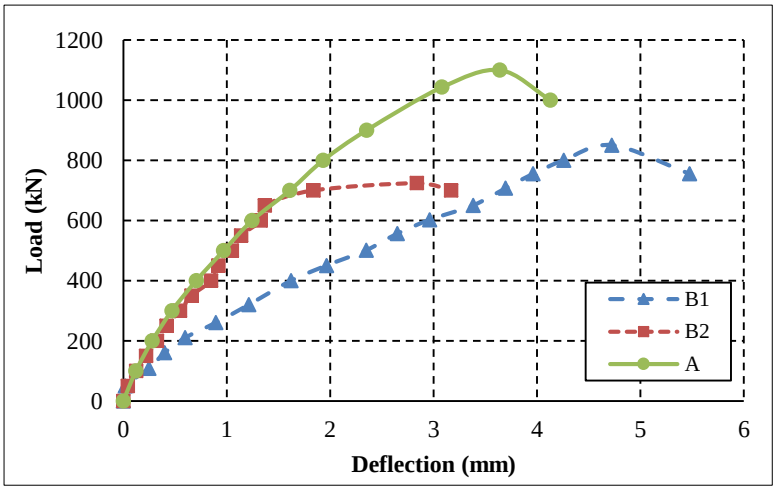

Figure 11. Load deflection curves for group B

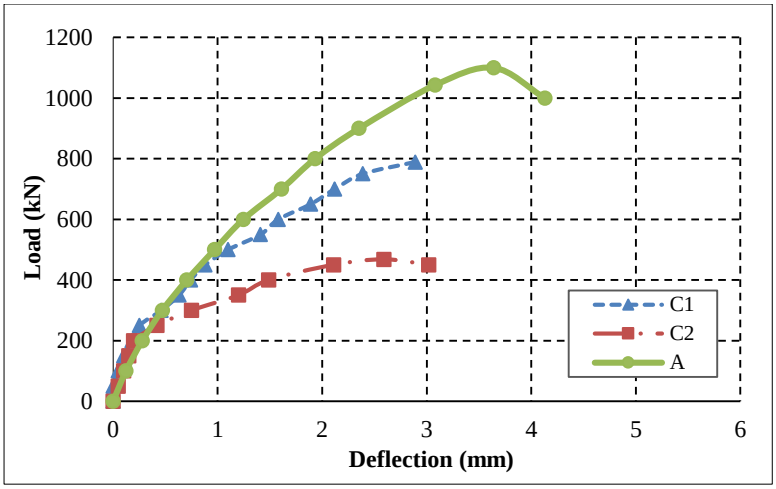

Figure 12. Load deflection curves for group C

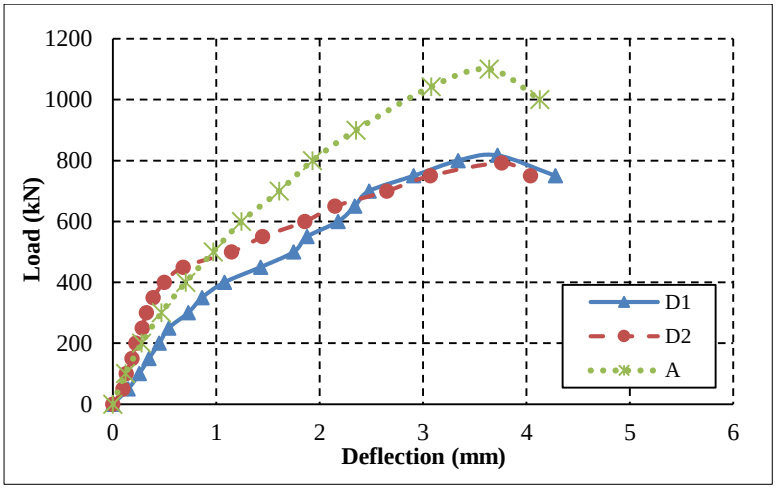

Figure 13. Load deflection curves for group D

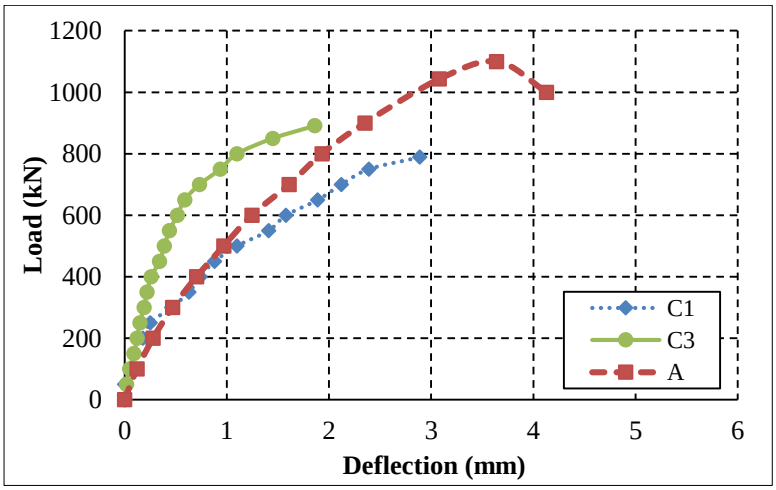

Figure 14. Load deflection curves for Beams C1 and C3

The location and size of the web opening affected the ultimate capacity and the deflection at ultimate load of the beams. For small openings, Beam B1 with the opening located outside the strut area towards the support had the highest capacity compared to beams C1 and D1 and the lowest reduction in strength of 17% compared to the solid beam A. Beam C1 where the opening intercepted the compression strut had the lowest capacity. In case of large openings, the ultimate capacity was less than that of the beams with small opening. Beam D2 with the opening located towards the midspan had the highest capacity between the beams with large openings while beam C2 had the lowest load capacity among all beams with a reduction of 54.7% compared to the control specimen A. The reduction in shear strength was

30% for beam B2 and 23.4% for beam D2. Beam C3 showed a higher load capacity and stiffness compared to C1 which means that having the embedded strut diverted around the opening led to a higher stiffness for the deep beam. Regarding the deflection at midspan measured at the ultimate load, beam B1 showed the highest value of deflection with an increase of the reference beam A of 30% while beams in Group C showed the lowest deflection. The large deflection value for beam B1 can be due to the various diagonal cracks observed along the span of the beam and the splitting at the support which led to a much-reduced stiffness as mentioned before. For group D both beams D1 and D2 had a very similar load deflection curves which means that when having the opening at the inner side from the strut the effect of the opening size becomes insignificant.

Figures 15 and 16 summarize the above results. In case of small openings, the horizontal location of the opening had a slight effect on the ultimate capacity of the beams as shown in Figure 15. While in case of large openings a significant reduction was observed for the beam with the opening interrupting the embedded strut. The size of the opening did not have a significant effect on the ultimate capacity when the opening was located outside the strut zone towards the middle part of the beam (0.4L) while the effect of the opening size was much more present in case of the opening intercepting the compression strut (0.22L) as can be seen in Figure 16. Having small openings led to an overall behavior similar to the comparative solid beam and a smaller reduction in capacity.

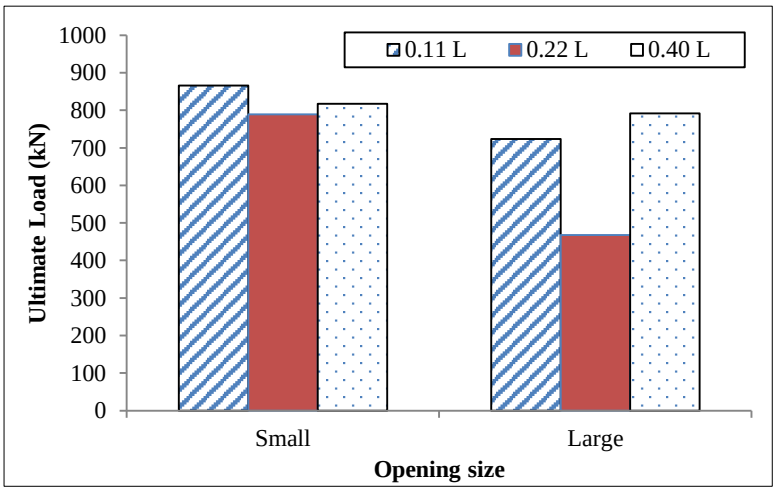

Figure 15. Effect of opening size

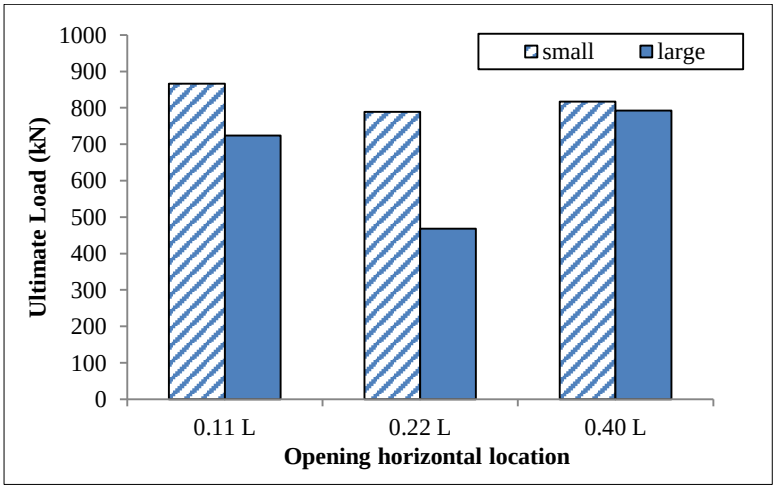

Figure 16. Effect of horizontal opening location

4.3. Strain in Reinforcing Bars

Figures 17 and 18 show the values of strain in the bottom and top longitudinal reinforcing bars of the specimens. The data recorded showed that the bottom reinforcement had tension strains throughout the loading and the top reinforcement had compression strains. For the bottom reinforcement none of the beams reached the yield strain with B1 experiencing the largest value of strain. Generally, beams with smaller opening had larger value of tensile strain in the longitudinal reinforcement in addition to group D where the opening was located at 0.4L. While C2 and B2 had the lowest values of strains. This means that the main tie reinforcement was not fully utilized for these two beams due to the location and large size of opening where failure occurred in the strut on the opening side. Comparing C1 and C3,

changing the strut reinforcement layout for beam C3 led to a higher value of strain in the bottom reinforcement. As for the top reinforcement, the beams showed rather small value of strains except for the reinforcement in beam A which reached the yield value.

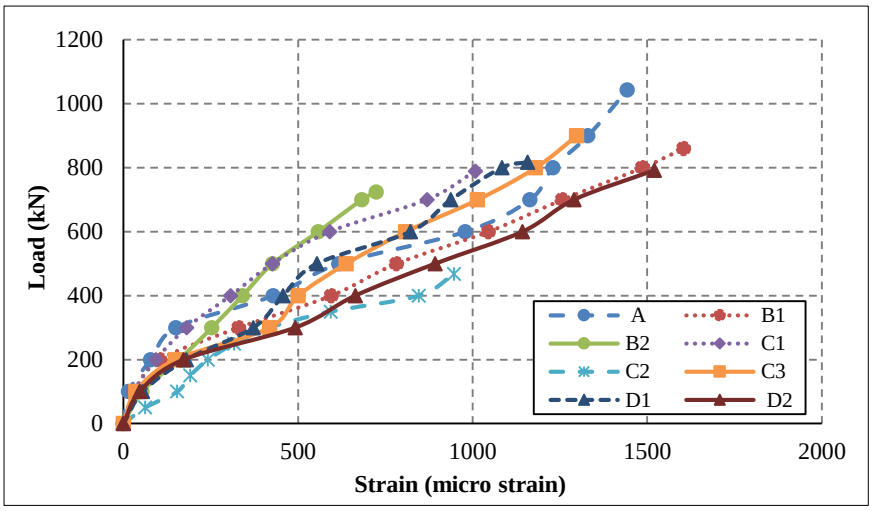

Figure 17. Load versus strain in bottom steel for all testes beams

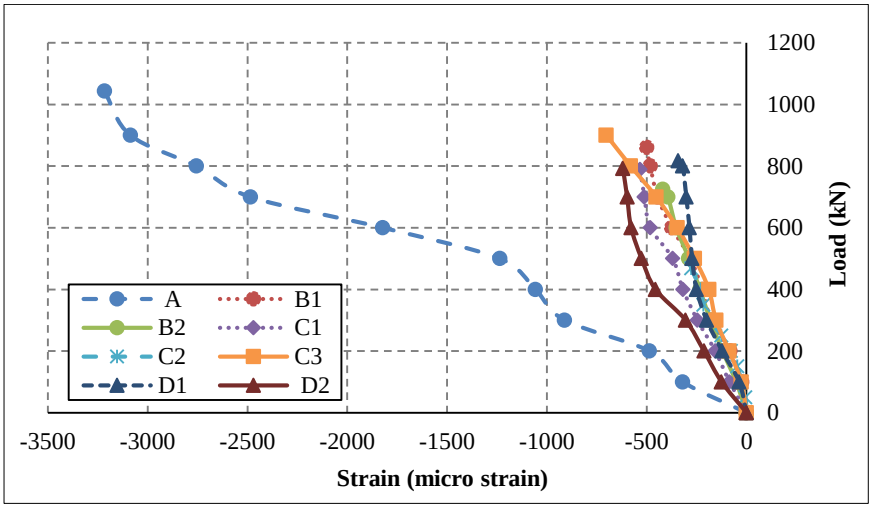

Figure 18. Load versus strain in top steel for all tested beams

5. Finite Element Modeling

There are currently no guidelines for the design and estimation of the ultimate capacity of deep beams with opening available in the codes of practice. The aim of this part of the research is to assess the feasibility of using the finite element analysis program, ANSYS 16 [39], to predict the behavior of deep beams with opening. An analytical analysis was conducted which consisted of two stages; the first one is model verification where the eight deep beams that were experimentally tested were modeled and analyzed using the ANSYS 16 program. The results of the analysis and experimental data were compared in terms of cracking pattern and ultimate load to ensure the validity of the model used. The second stage comprised of conducting a parametric study on additional six beams to investigate the effect of two more parameters, namely the reinforcement arrangement and the additional reinforcing bars around the opening.

5.1. Modeling Methodology

There are different types of elements within the ANSYS 16 library [39]. To accurately represent the concrete in finite element programs, nonlinear analysis needs to be used. The elements from the ANSYS 16 library [39] were selected to represent the nonlinear behavior of concrete. Three of these elements were used to model each item in the deep beam specimens. Solid 65 is the element used for 3D modeling of concrete as this element can show cracking in tension and crushing in compression as well as creep and plastic deformation. The element is defined by six faces and eight nodes, each node has three degrees of freedom: translations in the x, y and z directions. A schematic of the element is shown in Figure 19. The stress directions for the element solid 65 are parallel to the element coordinate system.

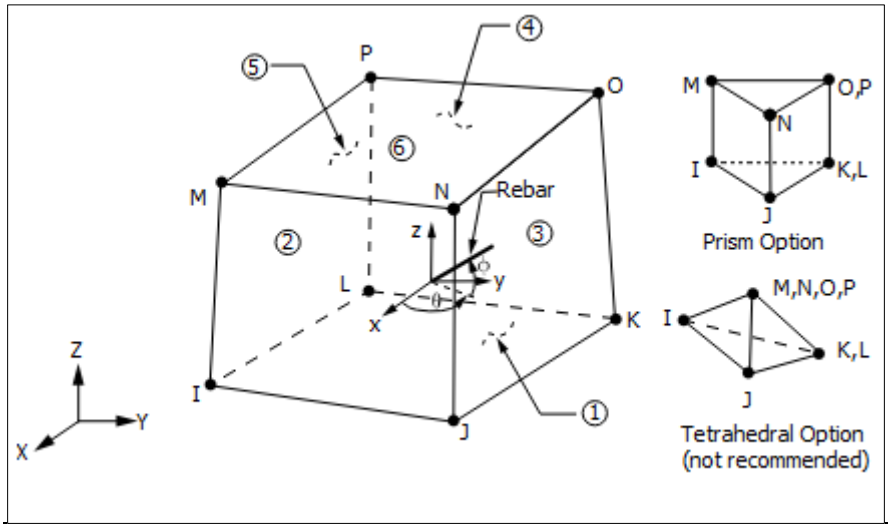

Figure 19. Solid 65 elements, ANSYS Theory [39]

Solid 45 element is used for 3D modeling of solid structures. It has eight nodes having three degrees of freedom at each node. This element is used to represent load plate and supports. The element has plasticity, creep, swelling, stress stiffening, large deflection, and large strain capabilities. The schematic of the element solid 45 is shown in Figure 20. Link 180 is an element used for 3D modeling of reinforcing bars. It is a uniaxial compression-tension element with two nodes, each node has three degrees of freedom: translations in the x, y, and z directions. It also includes plasticity, stress stiffness, creep, and large deflection and strain capabilities. This element is shown in Figure 21.

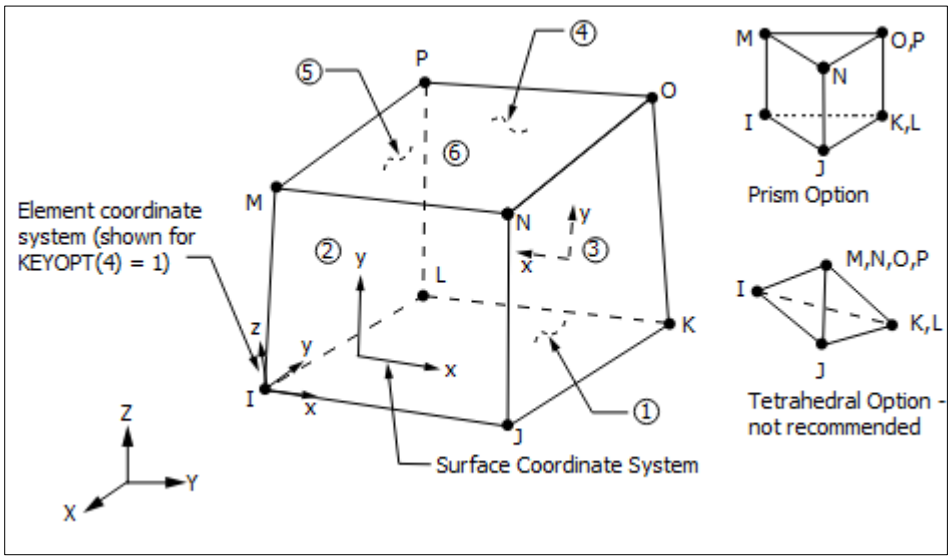

Figure 20. Solid 45 element [39]

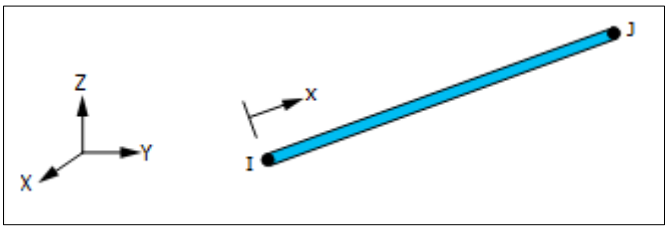

Figure 21. Link180 element [39]

5.2. Material Properties

Concrete has a different behavior in tension than in compression as well as being a brittle material. To model concrete in ANSYS [39], linear isotropic and multilinear isotropic as well as some additional properties are required to simulate the concrete behavior. The actual material properties obtained from laboratory testing were used as an input in the

numerical analysis. The material properties used in modeling were: the ultimate cubic compressive strength of concrete equal to 35 MPa and the corresponding modulus of elasticity of the concrete (E_C) equals 26590 MPa. Also, the tensile strength was taken as 3.8MPa and Poisson's ratio equal to 0.2. The shear transfer coefficient (β_t) represents the condition of the cracks face and it ranges from 0.0 to 1.0. When the shear transfer coefficient equals 0.0, the cracks are smooth representing complete loss of shear transfer and when the shear transfer coefficient equals 1.0 the cracks are rough where no loss of shear transfer occurs. The shear transfer coefficient for open and closed cracks was determined by Kachlakev and Miller [40]. The shear transfer coefficient is taken as 0.2 for open cracks and 0.8 for closed cracks.

To define the uniaxial compressive stress-strain curve for concrete, the numerical expressions proposed by Desayi and Krishnan [41] in Equations 1 and 2 as well as Equation 3 which was proposed by Gere and Timoshenko [42] were used. The Simplified compressive uniaxial stress-strain relationship used is shown in Figure 22. Typical high grade steel reinforcing bars was used to construct the steel reinforcement in the models. The steel for the finite elements models was assumed to be a bilinear isotropic, elastic-perfectly plastic material, and identical in tension and compression as shown in Figure 23. The steel plates were assumed as linear elastic material.

$$f = \frac{E_C\,\varepsilon}{1+(\frac{\varepsilon}{\varepsilon_0})^2} \quad (1)$$

$$\varepsilon_0 = \frac{2\,f_c'}{E_c} \quad (2)$$

$$E_c = \frac{f}{\varepsilon} \quad (3)$$

where *f is* stress at any strain ε, *ε is* stress at stress *f*, and ε_0 is strain at the ultimate compressive strength f_c'.

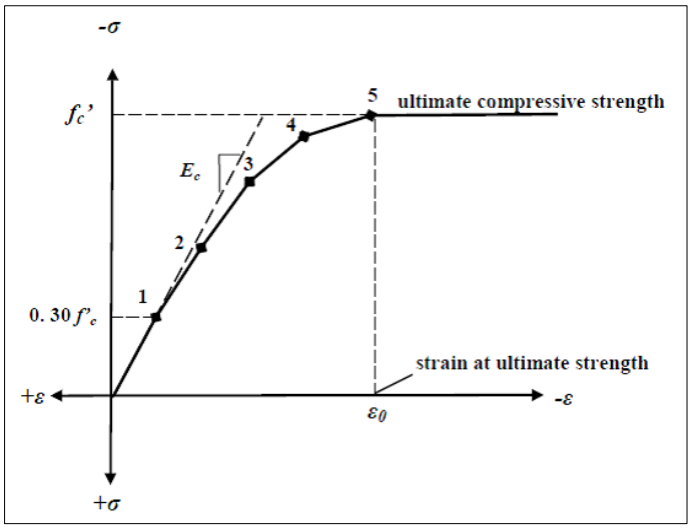

Figure 22. Uniaxial stress-strain curve for concrete model [41]

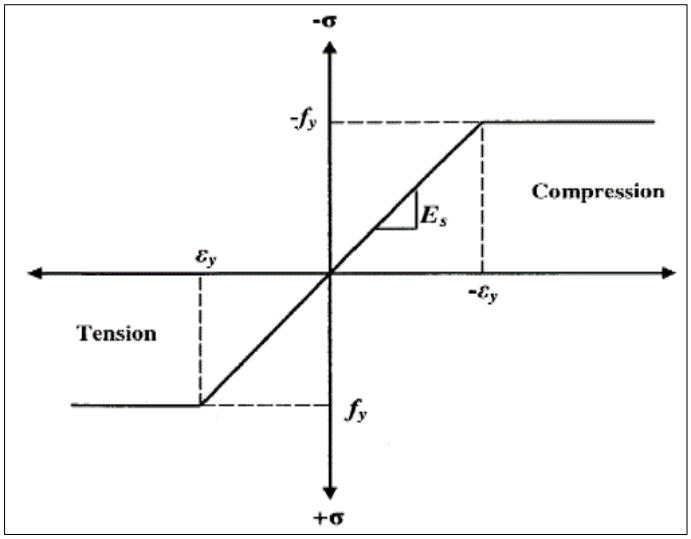

Figure 23. Stress-strain curve for steel reinforcement [43]

5.3. Meshing of the Analyzed Deep Beams

The beam mesh is selected such that the nodal points of the solid element coincide with the actual reinforcement locations. Additionally, nodal points were provided to subdivide the mesh, so that, a reasonable mesh density was obtained in the joint regions with the recommended aspect ratio of the element. Perfect bond between materials was assumed due to the limitations in ANSYS [39]. To provide a perfect bond, the link180 reinforcement element was connected between nodes of each adjacent solid 65 concrete elements, so the two materials shared the same nodes. Also, the solid 45 steel plate element was connected between nodes of each adjacent solid 65 concrete elements under point load. Figures 24 and 25 show the mesh of typical beam without and with opening, respectively.

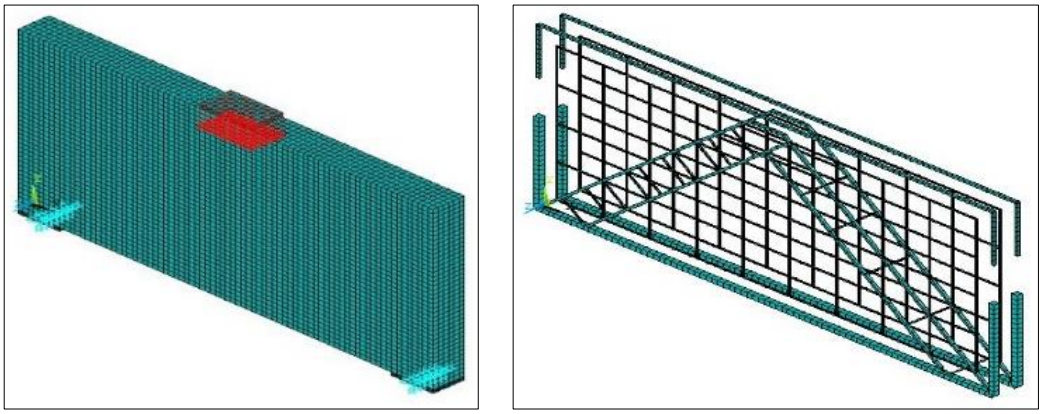

Figure 24. Mesh and model of deep beam without opening

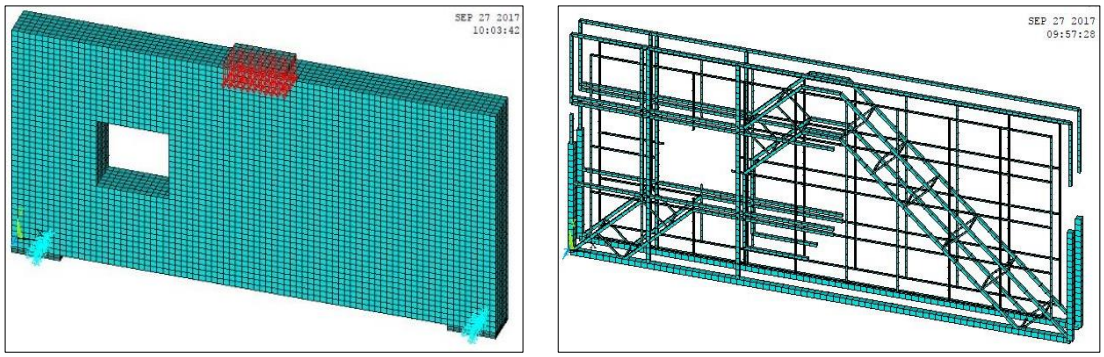

Figure 25. Mesh and model of typical beam with opening (300×300mm)

To ensure that the model acts the same way as the experimental beams, boundary conditions need to be applied at supports resembling the actual conditions during loading. Thus, the supports were modeled to give a hinged support where the value of the displacement for X and Y directions were set to zero for the node at each support. Figure 26 shows the modeling procedure where the load was applied as a vertical load at the top middle of the beam. Loading steps was divided into very small sub-steps to avoid non-convergence.

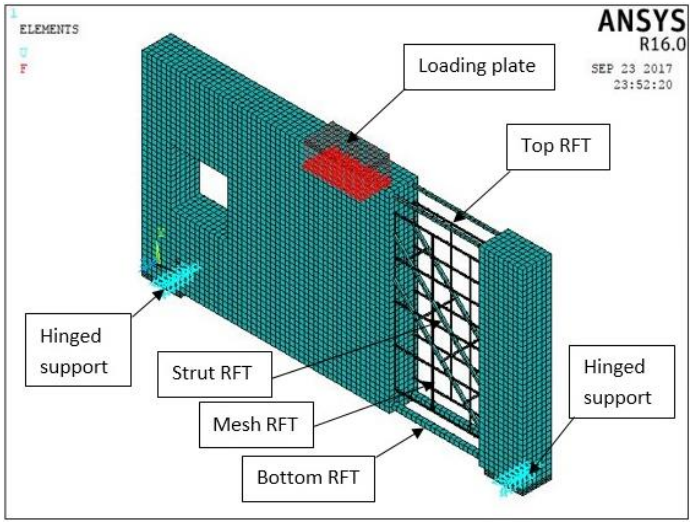

Figure 26. Boundary conditions used for the specimens

5.4. Verification of the Analytical Model

The validity of finite element modeling using ANSYS 16 [39] was first checked through comparison with the experimental test results. The eight beams A, B1, B2, C1, C2, C3, D1, and D2 were modeled and analyzed using the ANSYS 16 program as discussed in the previous sections. Table 3 shows the results of both the analysis and experiment in terms of first cracking and ultimate loads. The cracking patterns for the eight beams as obtained through ANSYS 16 are shown in Figures 27 to 29.

Table 3. Comparison between the experimental and numerical results of the tested specimens

Group	Beam	Opening size	Horizontal opening location	Experiment (kN)		ANSYS (kN)		P_{crA}/P_{crE} %	P_{uA}/P_{uE} %
				P_{crE}	P_{uE}	P_{crA}	P_{uA}		
A	A	-	-	550	1043	520	960	94.5 %	92.04 %
B	B1	150*150	0.11 L	385	866	420	820	109 %	94.70 %
	B2	300*300	0.11 L	320	724	350	610	109 %	84.25 %
C	C1	150*150	0.22 L	420	789	450	680	107 %	86.20 %
	C2	300*300	0.22 L	240	468	390	460	162.5 %	98.30 %
	C3	150*150	0.22 L	400	891	455	790	113.8 %	88.70 %
D	D1	150*150	0.40 L	385	817	500	720	130 %	88.15 %
	D2	300*300	0.40 L	350	792	430	710	122.9 %	89.65 %

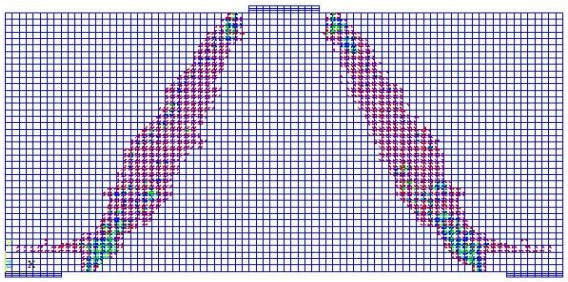

Figure 27. Cracking pattern at failure according to ANSYS 16 modeling for beam A

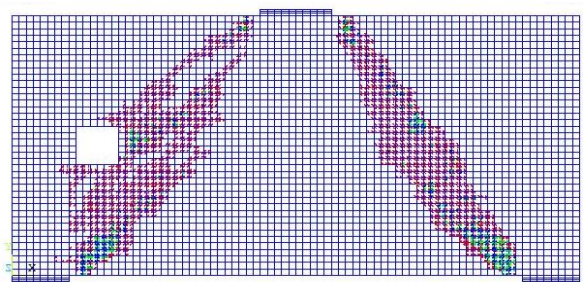

(a) Beam B1

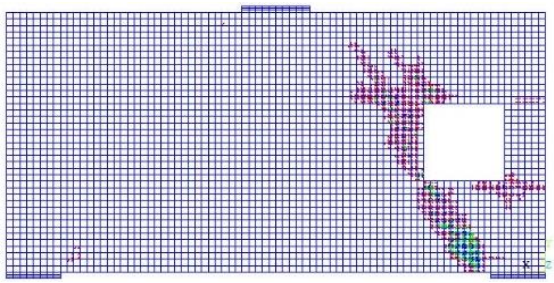

(b) Beam B2

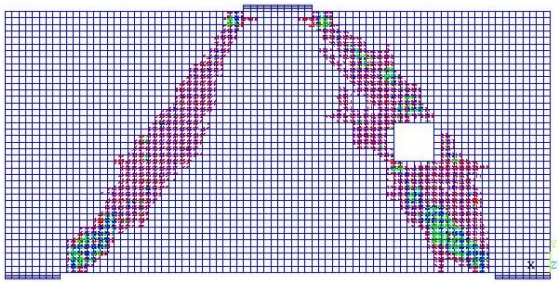

(c) Beam C1

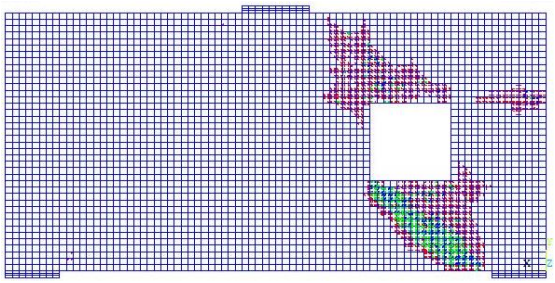

(d) Beam C2

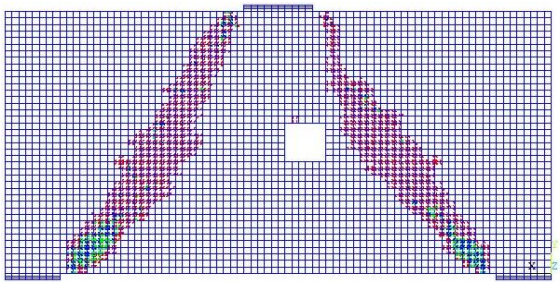

(e) Beam D1

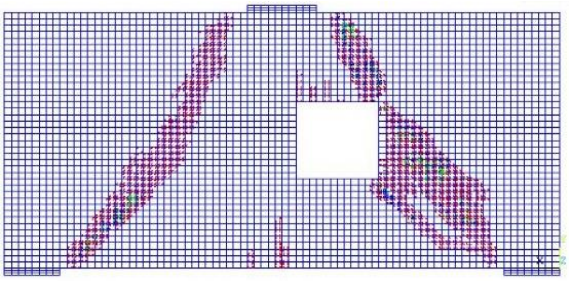

(f) Beam D2

Figure 28. Cracking pattern at failure according to ANSYS 16 modeling for Groups B, C and D

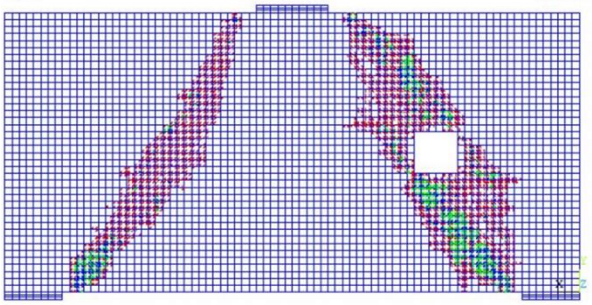

Figure 29. Cracking pattern at failure according to ANSYS 16 modeling for beam C3

Comparing the loads obtained from the analytical model to those obtained from the test results, the values of the first crack loads computed using ANSYS 16 was generally higher than the experiment except for beam A. However, the ultimate load was lower than the experiment with a maximum difference of 15.75 %. This difference can be attributed to some of the idealizations assumed during modeling such as the perfect bond between concrete and steel. However, since the values obtained using ANSYS were on the conservative side, this difference in values presents an acceptable value for numerical calculation. Comparing Figures 8 to 10 showing the experimental cracking patterns with Figures 27 to 29 showing the analytical ones, the cracking patterns using the analytical program were in good correlation with the experimental ones regarding the overall pattern and the failure mode. The only drawback was that the ANSYS 16 program did not very well capture the flexural cracks that were observed during the experiment. Based on this, it can be said that the model using the ANSYS 16 program can reasonably predict the behavior and the ultimate capacity of the deep beams with opening and thus can be used to further investigate different parameters that can affect the deep beams behavior.

6. Parametric Study

A parametric study was performed using the finite element analysis program (ANSYS 16) [39]. Two parameters were investigated namely, reinforcement arrangement across the beam web and strengthening reinforcement around the openings. The outline of the parameters and the specimens are shown in Table 4. Table 5 and Figures 30 and 31 show the details of the specimens used. In this part, two more groups are added. Group E having specimen E1 and E2 where the reinforcement arrangement in these two specimens was taken as the conventional orthogonal mesh using high grade steel with a value of 5 Ø 16/m each face corresponding to a reinforcement ratio of 1.34%. E1 was a solid beam while E2 had an opening with size 300×300 mm located at 0.22 L. These two specimens will be compared with beams A and C2 previously tested and analytically modeled. The dimensions and the top and bottom reinforcement are taken as beams A and C2. The size and location of the opening is chosen here as the most critical one which corresponds to beam C2. The second group is Group F composed of four beams to be compared with beam C2. In this group of beams, the additional reinforcement bars around the opening were varied as shown in Table 5 from two bars with diameter 8 mm to two bars with diameter 18 using mild steel. Table 6 shows the first crack and ultimate loads for the beams in groups E and F.

Table 4. Outline of parametric study program

Group	Specimen number	Comparative Specimen	Parameter under study
E	E1, E2	A, C2	Mesh reinforcement against embedded strut arrangement
F	F1, F2, F3, F4	C2	Value of additional reinforcement around opening

Table 5. Details of specimens used in the parametric study

Group	Specimen number	Dimensions (mm)	Mesh reinforcement		Opening details			
			Rft. / Each face	Fy (N/mm^2)	Opening size (mm)	Opening CL. HZ. location	Opening CL. VL. location	Rft. around opening / each face
E	E1	2000*1000*150	5 Ø 16/m	360	-	-	-	-
	E2		5 Ø 16/m	360	300*300	0.22 L	0.5 h	2 Ø 12
F	F1		5 Ø 6/m	240	300*300	0.22 L	0.5 h	2 Ø 18
	F2		5 Ø 6/m	240	300*300	0.22 L	0.5 h	2 Ø 16
	F3		5 Ø 6/m	240	300*300	0.22 L	0.5 h	2 Ø 10
	F4		5 Ø 6/m	240	300*300	0.22 L	0.5 h	2 Ø 8
Comparative Specimen	A		5 Ø 6/m	240	-	-	-	-
	C2		5 Ø 6/m	240	300*300	0.22 L	0.5 h	2 Ø 12

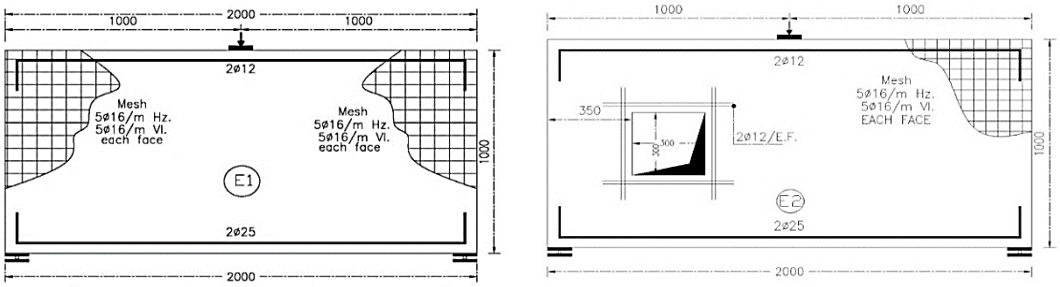

Figure 30. Geometry and reinforcement details of beams E1 and E2

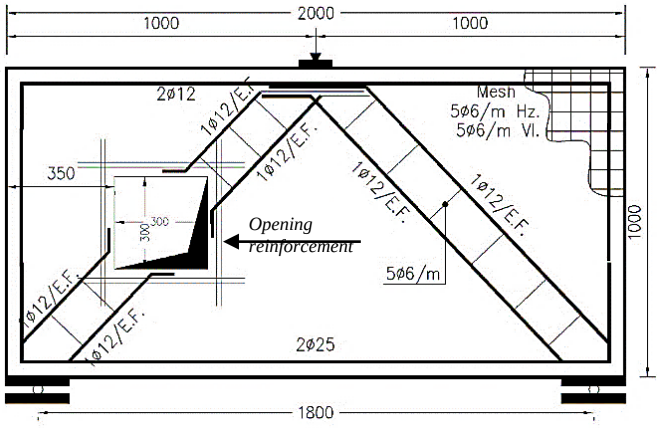

Figure 31. Geometry and reinforcement details of the deep beams in Group F

Table 6. Cracking and ultimate numerical results for Groups E and F

Group	Beam	P_{cr} (KN)	Pu (KN)
A	A	520	960
C	C2	260	460
E	E1	580	1050
	E2	265	590
F	F1	265	510
	F2	265	500
	F3	260	450
	F4	260	425

5.3.1. Group E

Table 6 shows the first crack and ultimate loads for the beams in groups E and F. The values of the ultimate load slightly increased for beam E1 compared to beam A, while beam E2 showed an increase of 28.2% over beam C2. Using orthogonal mesh reinforcement with a ratio of 1.34% showed improved results over the embedded strut layout especially in case of the beam with opening directly interrupting the compression strut path. The cracking patterns were similar as well as the load deflection behavior for the four beams as shown in Figures 32 to 34.

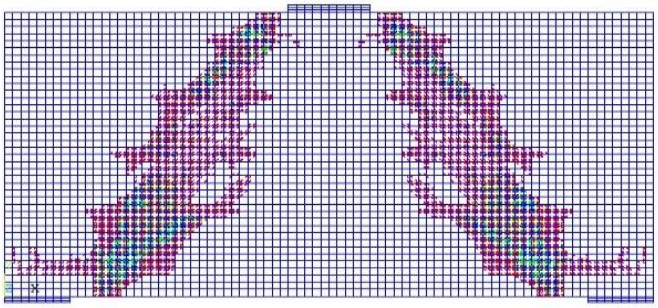

Figure 32. Numerical cracking pattern for Beam E1

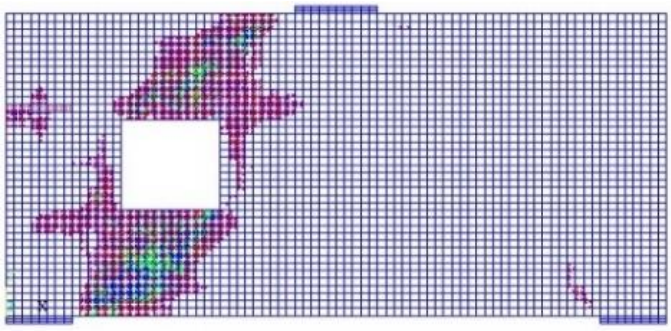

Figure 33. Numerical cracking pattern for Beam E2

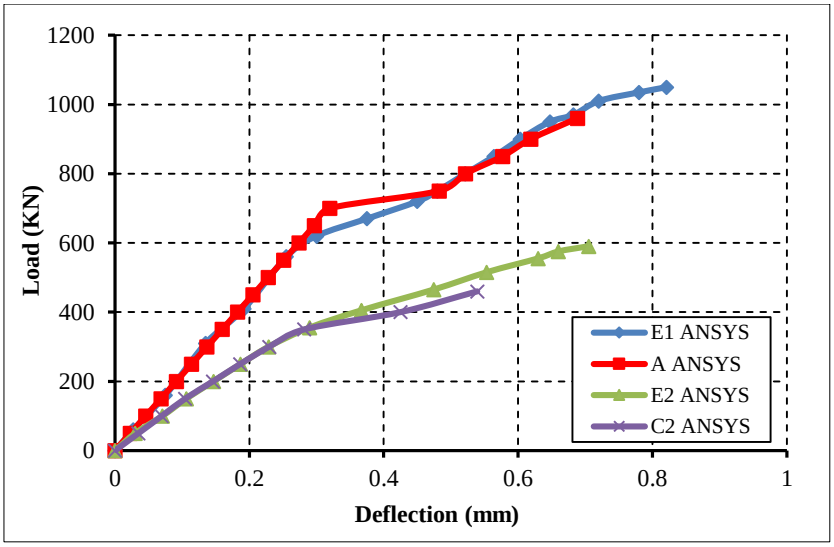

Figure 34. Load deflection curves for group E compared to beam A and C2 (according to ANSYS)

5.3.2. Group F

Comparing the cracking patterns for group F in Figure 35, in addition to beam C2 in Figure 28d, the stresses around the opening increased as the amount of additional reinforcement increased. The amount of additional reinforcement affects the behavior of the beam where the strut pattern above and below the opening is clearer as the amount of reinforcement increases. The five beams presented very similar load deflection behavior as seen in Figures 36. From Figure 37, the value of the ultimate load increased by 20% when the bar diameter was changed from 8 mm to 18 mm.

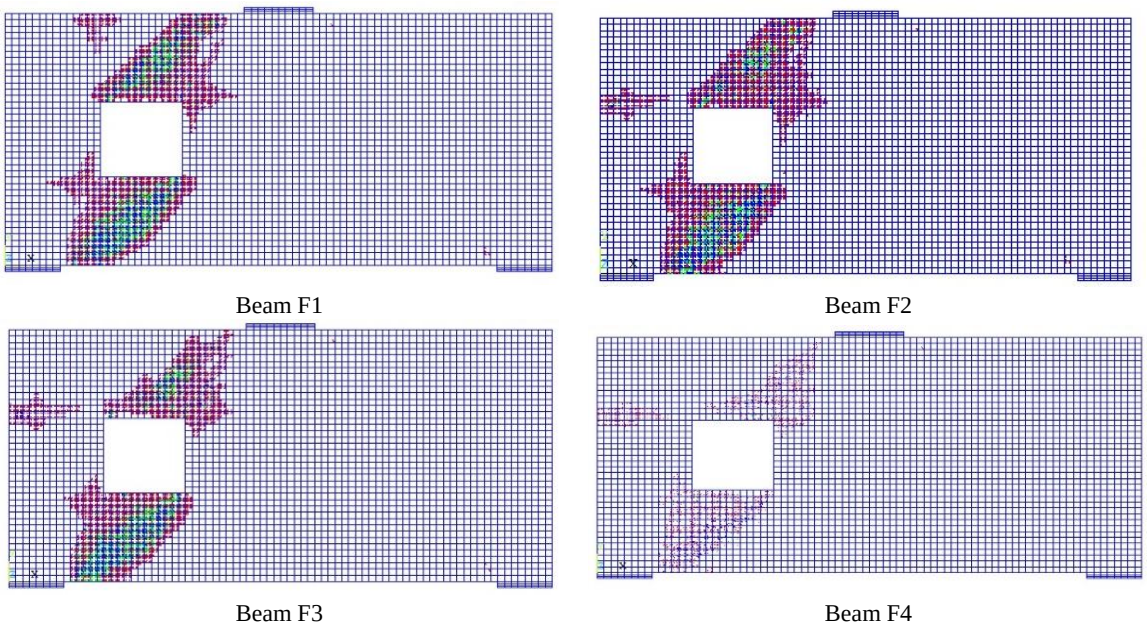

Figure 35. Numerical cracking patterns at failure for group F

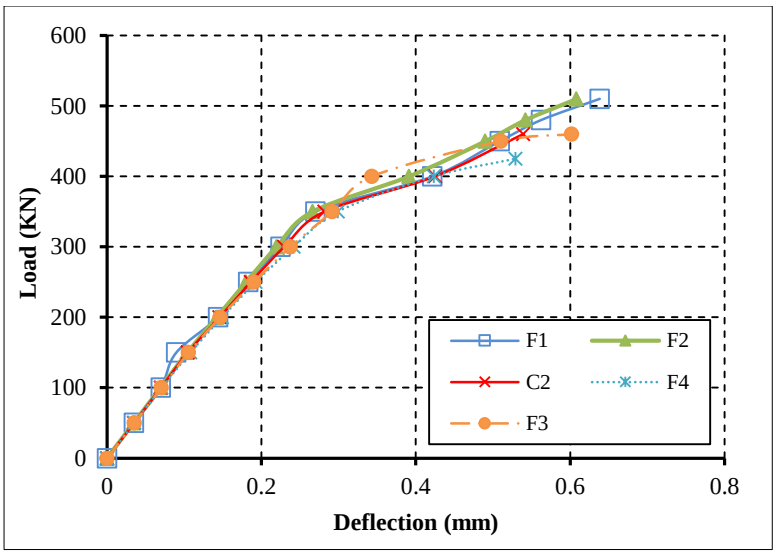

Figure 36. Load deflection for group F and beam C2 according to ANSYS

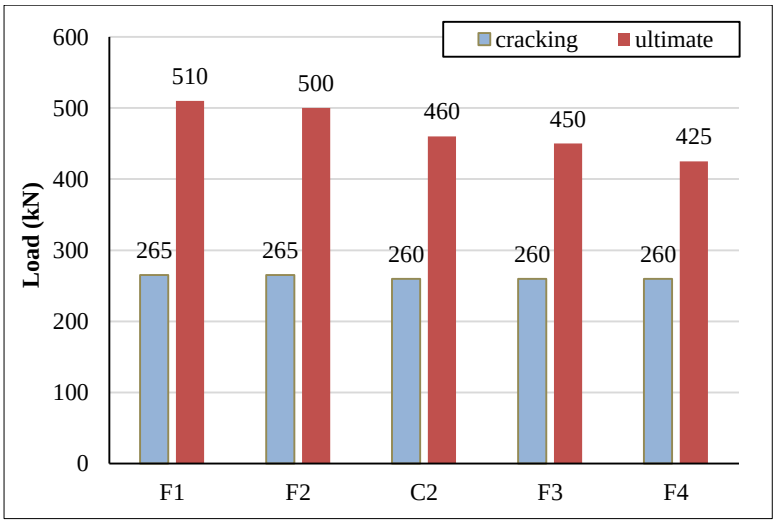

Figure 37. Cracking and ultimate numerical results for group F and beam C2

7. Conclusions

The aim of this study is to investigate the effect of the size and location of opening and the arrangement of reinforcement using embedded struts on the structural behavior of RC deep beams subjected to concentrated load at mid-span. Experimental tests were carried out on eight deep beams with and without openings having the same dimensions. A numerical FEA study using the ANSYS program was conducted to investigate the behavior of the tested deep beams. The results of the numerical models were compared with those obtained from the experimental work. The analytical results were found to be in good agreement with the experimental results. In addition, a parametric study was conducted to further assess the effect of increasing reinforcement around the opening and using the conventional mesh reinforcement to match that in the shape of the embedded strut and tie. The following conclusions may be drawn:

- For the large-opening beams that were tested, the first cracks showed up at the diagonal corners of the opening and were at an angle of about 45 degrees to the beam's longitudinal axis.
- The mode of failure depended on the opening size rather than the location of the openings, where for large openings, compression occurred along the lines from the corners of the opening towards the loading point and the support. For small openings, failure occurred along the main compression strut.
- The load-deflection relationship for RC deep beams was linear up to the cracking load and nonlinear after. The slope of the curves after cracking decreased, indicating a reduction of the beam stiffness after cracking.
- The location of the opening did not significantly affect the strength of the beam in the case of small openings but had a pronounced effect in the case of large openings. In fact, the deep beams with small web openings behaved very similarly to the solid reference beam.

- A larger reduction in beam capacity was observed with the large openings, and the most significant was observed when the opening directly interrupted the compression strut at 0.22 of the clear span length. The beams with small openings located towards the middle of the beam with a ratio of 0.4 of the clear span had the lowest reduction in capacity. Thus, it can be recommended to have small web openings towards the middle of the beams for the least effect on the beam behavior.
- Diverting the strut reinforcement layout around the opening improved the beam capacity.
- The analytical results obtained from (ANSYS 16) agree well with the experimental results in terms of crack pattern as well as the ultimate load values, which showed differences of within 20% compared to the experimental values, which means that ANSYS can be a reasonable tool used in the analysis of deep beams with opening.
- Changing the reinforcement layout to orthogonal mesh caused an increase in the beam capacity in the case of the beams with openings and almost no change in the case of solid beams.
- The increase in the value of the additional reinforcement around the opening caused a slight increase in the capacity of the beam.
- The study showed that using embedded struts in the case of deep beams with openings can be a suitable method for the reinforcement arrangement along the web of the beam. However, more research is still needed with different strut layouts and variable reinforcement ratios for the strut, web reinforcement, and the additional reinforcement around the openings.

8. Declarations

8.1. Author Contributions

The main ideas and the methodology of the research were discussed and decided by all the authors. The manuscript was written by M.M. and R.M. and the review was done by M.K. The results, discussions, interpretation, and conclusion were completed by all authors. All authors have read and agreed to the published version of the manuscript.

8.2. Data Availability Statement

The data presented in this study are available in the article.

8.3. Funding

The authors received no financial support for the research, authorship, and/or publication of this article.

8.4. Conflicts of Interest

The authors declare no conflict of interest.

9. References

[1] ACI 318-19. (2019). Building Code Requirements for Structural Concrete (ACI 318-19) and Commentary (ACI 318R-19). American Concrete Institute (ACI), Farmington Hills, United States. doi:10.14359/51716937.

[2] ECP 203-2007. (2007). Egyptian Code for the Design and Construction of concrete Structures, Housing and Building Research Centre, Ministry of Housing, Utilities and Urban Communities, Cairo, Egypt.

[3] Wight J. K., & MacGregor J. G. (2011). Reinforced Concrete Mechanics and Design (6th Ed.). Pearson Prentice Hall, Hoboken, United States.

[4] EN 1992-1-1. (2004). Eurocode 2: Design of Concrete Structures, Part 1-1: General Rules and Rules for Buildings. European Committee for Standardization, Brussels, Belgium.

[5] The international Federation for Structural Concrete (fib). (2013). fib Model Code for Concrete Structures 2010. John Wiley & Sons, New Jersey, United States.

[6] CSA A23.3:19. (2019). Design of Concrete Structures, Standards Council of Canada, Ottawa, Canada.

[7] Tan, K. H., Dong, F. K., & Weng, L. W. (1998). High-strength reinforced concrete deep and short beams: shear design equations in North American and UK practice. Structural Journal, 95(3), 318-329. doi:10.14359/549.

[8] Hwang, S. J., Lu, W. Y., & Lee, H. J. (2000). Shear strength prediction for deep beams. Structural Journal, 97(3), 367-376. doi:10.14359/9624.

[9] Salami, M. R., Kobayashi H., & Unjoh, S. h. (2005). Experimental and Analytical Study on RC Deep Beams. Asian Journal of Civil Engineering (Building and Housing), 6(5), 409-421.

[10] Dalaf, A. N., & Mohammed, S. D. (2021). Steel Fiber Enhancement upon Punching Shear Strength of Concrete Flat Plates Exposed to Fire Flame. Civil Engineering Journal, 7(10), 1667–1678. doi:10.28991/cej-2021-03091751.

[11] Quintero-Febres, C. G., Parra-Montesinos, G., & Wight, J. K. (2006). Strength of struts in deep concrete members designed using strut-and-tie method. ACI Structural Journal, 103(4), 577–586. doi:10.14359/16434.

[12] Kondalraj, R., & Appa Rao, G. (2021). Experimental verification of ACI 318 strut-and-tie method for design of deep beams without web reinforcement. ACI Structural Journal, 118(1), 139–152. doi:10.14359/51728083.

[13] El-Zoughiby, M. (2021). Load-Spread Spectrum in Strut-and-Tie Modeling of Structural Concrete. ACI Structural Journal, 118(4), 3–15. doi:10.14359/51732639.

[14] Hwang, S. J., Yang, Y. H., & Li, Y. A. (2021). Maximum shear strength of reinforced concrete deep beams. ACI Structural Journal, 118(6), 155–164. doi:10.14359/51733076.

[15] Lee, J. Y., & Kang, Y. M. (2021). Strut-and-tie model without discontinuity for reinforced concrete deep beams. ACI Structural Journal, 118(5), 123–134. doi:10.14359/51732824.

[16] Kong, F. K., & Sharp, G. R. (1977). Structural idealization for deep beams with web openings. Magazine of Concrete Research, 29(99), 81-91. doi:10.1680/macr.1977.29.99.81.

[17] Kong, F. K., Sharp, G. R., Appleton, S. C., Beaumont, C. J., & Kubik, L. A. (1978). Structural idealization for deep beams with web openings: further evidence. Magazine of Concrete Research, 30(103), 89-95. doi:10.1680/macr.1978.30.103.89.

[18] Almeida, A. P., & De Oliveira Pinto, N. (1999). High-strength concrete deep beams with web openings. American Concrete Institute, ACI Special Publication, SP186, 597–613. doi:10.14359/5580.

[19] Maxwell, B. S., & Breen, J. E. (2000). Experimental evaluation of strut-and-tie model applied to deep beam with opening. Structural Journal, 97(1), 142-148. doi:10.14359/843.

[20] Eun, H. C., Lee, Y. H., Chung, H. S., & Yang, K. H. (2006). On the shear strength of reinforced concrete deep beam with web opening. Structural Design of Tall and Special Buildings, 15(4), 445–466. doi:10.1002/tal.306.

[21] Mau, S. T., & Hsu, T. T. (1987). Shear strength prediction for deep beams with web reinforcement. Structural Journal, 84(6), 513-523. doi:10.14359/2739.

[22] Ley, M. T., Riding, K. A., Bae, S., & Breen, J. E. (2007). Experimental verification of strut-and-tie model design method. ACI Structural Journal, 104(6), 749-755. doi:10.14359/18957.

[23] Garber, D. B., Gallardo, J. M., Huaco, G. D., Samaras, V. A., & Breen, J. E. (2014). Experimental evaluation of strut-and-tie model of indeterminate deep beam. ACI Structural Journal, 111(4), 873–880. doi:10.14359/51686738.

[24] Brena, S. F., & Morrison, M. C. (2007). Factors affecting strength of elements designed using strut-and-tie models. ACI Structural Journal, 104(3), 267. doi:10.14359/18616.

[25] Zhou, M., Zhong, J. T., Wang, L., & Chen, H. T. (2021). Application of evaluation system for strut-and-tie models of reinforced concrete structures. ACI Structural Journal, 118(1), 17–30. doi:10.14359/51728088.

[26] Vaquero, S. F., & Bertero, R. D. (2020). Automatic generation of proper strut-and-tie model. ACI Structural Journal, 117(6), 81–92. doi:10.14359/51725905.

[27] El-Zoughiby, M. E. (2021). Z-Shaped Load Path: A Unifying Approach to Developing Strut-and-Tie Models. ACI Structural Journal, 118(3), 35-48. doi:10.14359/51730535.

[28] Tan, K. H., Tong, K., & Tang, C. Y. (2003). Consistent strut-and-tie modelling of deep beams with web openings. Magazine of Concrete Research, 55(1), 65–75. doi:10.1680/macr.2003.55.1.65.

[29] Ashour, A. F., & Rishi, G. (2000). Tests of reinforced concrete continuous deep beams with web openings. Structural Journal, 97(3), 418-426. doi:10.14359/4636.

[30] Campione, G., & Minafò, G. (2012). Behaviour of concrete deep beams with openings and low shear span-to-depth ratio. Engineering Structures, 41, 294–306. doi:10.1016/j.engstruct.2012.03.055.

[31] Frappier, J., Mohamed, K., Farghaly, A. S., & Benmokrane, B. (2019). Behavior and strength of glass fiber-reinforced polymer-reinforced concrete deep beams with web openings. ACI Structural Journal, 116(5), 275–286. doi:10.14359/51716774.

[32] Yang, K. H., Chung, H. S., & Ashour, A. F. (2007). Influence of inclined web reinforcement on reinforced concrete deep beams with openings. ACI Structural Journal, 104(5), 580–589. doi:10.14359/18860.

[33] Yang, K. H., & Ashour, A. F. (2008). Effectiveness of web reinforcement around openings in continuous concrete deep beams. ACI Structural Journal, 105(4), 414–424. doi:10.14359/19855.

[34] Jasim, W. A., Allawi, A. A., & Ali Oukaili, N. K. (2019). Effect of Size and Location of Square Web Openings on the Entire Behavior of Reinforced Concrete Deep Beams. Civil Engineering Journal, 5(1), 209. doi:10.28991/cej-2019-03091239.

[35] Starčev-Ćurčin, A., Rašeta, A., Malešev, M., Kukaras, D., Radonjanin, V., Šešlija, M., & Žarković, D. (2020). Experimental Testing of Reinforced Concrete Deep Beams Designed by Strut-And-Tie Method. Applied Sciences, 10(18), 6217. doi:10.3390/APP10186217.

[36] Ibrahim, M. A., El Thakeb, A., Mostfa, A. A., & Kottb, H. A. (2018). Proposed formula for design of deep beams with shear openings. HBRC Journal, 14(3), 450–465. doi:10.1016/j.hbrcj.2018.06.001.

[37] Tseng, C. C., Hwang, S. J., & Lu, W. Y. (2017). Shear strength prediction of reinforced concrete deep beams with web openings. ACI Structural Journal, 114(6), 1569–1579. doi:10.14359/51700950.

[38] Lafta, Y. J., & Ye, K. (2016). Specification of deep beams affect the shear strength capacity. Civil and Environmental Research, 8(2), 56–68.

[39] ANSYS Theory Reference Release 5.6. (1999). ANSYS, Inc., Pennsylvania, United States.

[40] Kachlakev, D., Miller, T. R., Yim, S., Chansawat, K., & Potisuk, T. (2001). Finite element modeling of concrete structures strengthened with FRP laminates. Technical report, FHWA-OR-RD-01-17. Oregon Department of Transportation: Research Section, Salem, United States.

[41] Desayi, P., & Krishnan, S. (1964). Equation for the Stress-Strain Curve of Concrete. Journal Proceedings, 61(3), 345–350. doi:10.14359/7785.

[42] Fanning, P. (2001). Nonlinear models of reinforced and post-tensioned concrete beams. Electronic Journal of Structural Engineering, 1(2), 111–119.

[43] Tavarez, F.A., (2001). Simulation of Behavior of Composite Grid Reinforced Concrete Beams Using Explicit Finite Element Methods. Master's Thesis, University of Wisconsin-Madison, Madison, United States.